AFRL-SN-RS-TR-2007-145
Final Technical Report
May 2007

WIDEBAND ELECTROABSORPTION MODULATOR FOR ANALOG APPLICATIONS

University of California at San Diego

AIR FORCE RESEARCH LABORATORY
SENSORS DIRECTORATE
ROME RESEARCH SITE
ROME, NEW YORK

NOTICE AND SIGNATURE PAGE

Using Government drawings, specifications, or other data included in this document for any purpose other than Government procurement does not in any way obligate the U.S. Government. The fact that the Government formulated or supplied the drawings, specifications, or other data does not license the holder or any other person or corporation; or convey any rights or permission to manufacture, use, or sell any patented invention that may relate to them.

This report was cleared for public release by the Air Force Research Laboratory Rome Research Site Public Affairs Office and is available to the general public, including foreign nationals. Copies may be obtained from the Defense Technical Information Center (DTIC) (http://www.dtic.mil).

AFRL-SN-RS-TR-2007-145 HAS BEEN REVIEWED AND IS APPROVED FOR PUBLICATION IN ACCORDANCE WITH ASSIGNED DISTRIBUTION STATEMENT.

FOR THE DIRECTOR:

/s/

JAMES R. HUNTER
Work Unit Manager

/s/

RICHARD G. SHAUGNESSY
Chief, Rome Operations Site
Sensors Directorate

This report is published in the interest of scientific and technical information exchange, and its publication does not constitute the Government's approval or disapproval of its ideas or findings.

REPORT DOCUMENTATION PAGE

Form Approved
OMB No. 0704-0188

1. REPORT DATE *(DD-MM-YYYY)*	2. REPORT TYPE	3. DATES COVERED *(From - To)*
MAY 2007	Final	Feb 06 – Feb 07

4. TITLE AND SUBTITLE

WIDEBAND ELECTROABSORPTION MODULATOR FOR ANALOG APPLICATIONS

5a. CONTRACT NUMBER

5b. GRANT NUMBER
FA8750-06-1-0055

5c. PROGRAM ELEMENT NUMBER
62500F

6. AUTHOR(S)

P.K.L. Yu, I. Shubin, X.B. Xie and W.S.C. Chang

5d. PROJECT NUMBER
WEMD

5e. TASK NUMBER
SN

5f. WORK UNIT NUMBER
01

7. PERFORMING ORGANIZATION NAME(S) AND ADDRESS(ES)
University of California at San Diego
9500 Gilman Dr. Dept 621
La Jolla CA 92093-5004

8. PERFORMING ORGANIZATION REPORT NUMBER

9. SPONSORING/MONITORING AGENCY NAME(S) AND ADDRESS(ES)

AFRL/SNDP
25 Electronic Pky
Rome NY 13441-4515

10. SPONSOR/MONITOR'S ACRONYM(S)

11. SPONSORING/MONITORING AGENCY REPORT NUMBER
AFRL-SN-RS-TR-2007-145

12. DISTRIBUTION AVAILABILITY STATEMENT
APPROVED FOR PUBLIC RELEASE; DISTRIBUTION UNLIMITED. PA# 07-253

13. SUPPLEMENTARY NOTES

14. ABSTRACT
There were two main technical objectives of this program with respect to the investigation of the high speed waveguide electroabsorption (EA) modulator, namely: (1) Design and fabrication of a waveguide modulator with a widened optical waveguide for easy packaging and lower insertion loss, and (2) interfacing with Infotonics for their fiber packaging effort of the modulator. In addition, an examination of the limits to Radio Frequency (RF) link gain, noise figure and spurious free dynamic range (SFDR) of the EA modulator was accomplished.
This program produced the following accomplishments: 1) Finished a design for the modulator with large optical waveguide to improve the coupling in materials structure of either bulk InGaAsP or multiple quantum wells. The design has been fabricated at UCSD and repeated at a commercial foundry. 2) Examined the limits of RF link gain, noise figure and SFDR of EA modulators.

15. SUBJECT TERMS
Optical modulator, Analog Optical Links, electroabsorption modulator, RF optical links

16. SECURITY CLASSIFICATION OF:			17. LIMITATION OF ABSTRACT	18. NUMBER OF PAGES	19a. NAME OF RESPONSIBLE PERSON
a. REPORT	b. ABSTRACT	c. THIS PAGE			James R. Hunter
U	U	U	UL	23	19b. TELEPHONE NUMBER (*Include area code*)

TABLE OF CONTENTS

LIST OF FIGURES

LIST OF TABLES

1. Technical Summary:

There were two main technical objectives of this program with respect to the investigation of the high speed waveguide electroabsorption (EA) modulator, namely: (1) Design and fabrication of a waveguide modulator with widened optical waveguide for easy packaging and lower insertion loss, and (2) interfacing with Infotonics for their fiber packaging effort of the modulator.

In addition, an examination of the limits to Radio Frequency (RF) link gain, noise figure and spurious free dynamic range (SFDR) of the EA modulator was accomplished.

This report[1] details the University of California at San Diego (UCSD) efforts in a multi-year collaborative research program with AFRL at Rome Research Site who evaluated the EA modulators in fiber links.

2. Introduction:

This program produced the following accomplishments:

1. Finished a design for the modulator with large optical waveguide to improve the coupling in materials structure of either bulk InGaAsP or multiple quantum wells. The design has been fabricated at UCSD and repeated at a commercial foundry. While the UCSD fabrication run has contact adhesion problem, the fabrication run at the commercial foundry has resolved this problem. The optical and electrical performances of devices fabricated at both locations are similar.
2. Examined the limits of RF link gain, noise figure and SFDR of EA modulators.

[1] The tasks reported in this project are also partially funded by program supported by DARPA and Air Force via Lockheed Martin.

3. Summary of accomplishments

3.1 High power diluted waveguide electroabsorption modulator

A diluted waveguide electroabsorption modulator using bulk InGaAsP electroabsorption layer has been designed and fabricated. The same design was transferred to a commercial foundry. The resulting devices achieved the same device properties as those fabricated at UCSD, with powers reaching 100 mW. A realistic and practical microwave equivalent circuit model was also developed which explains the S-parameters that were measured experimentally.

3.2 RF link gain and noise figure limits of electroabsorption modulator

In a collaborative effort with Photonic Systems Inc., the RF link limit and noise figure limit of electroabsorption modulator operating under optimal conditions has been theoretically and experimentally established. The photocurrent at the modulator results in a feedback effect that limits the available RF power reaching the modulator. This limits the maximum link gain and noise figure of links using the electroabsorption modulator.

3.3 Limit of Spurious free dynamic range of electroabsorption modulator

The spurious free dynamic range (SFDR) of electroabsorption modulator has been examined. The same current feedback mechanism that limits the RF link gain is found to be beneficial for the high SFDR operation.

4. Technical progress achieved on project.

4.1 High power diluted waveguide electroabsorption modulator

The basic device structure of the electroabsorption modulator investigated under this program is a continuation of the structure investigated under an Air Force program (Wideband Agile Modulator) at Lockheed Martin with a subcontract at UCSD. The frequency bandwidth is set at 20 GHz. The material structure is based upon the bandwidth and modulation efficiency requirements. Initially the substrate is n-type Indium Phosphide (InP) to ease the RF package requirements. It was later determined that there is a considerable problem with the metal bonding on the p-electrode on top of BCB. The recommendation (to the commercial foundry) was to make them on semi-insulating InP. Table 1 summarizes the original material layer structure on n-InP substrate design.

Table 1. Material Layer structure of the diluted core waveguide electroabsorption modulator. (The quaternary InGaAsP Q1.46 is the modulation layer; the Q1.15 is the waveguide layer, with bandgap wavelength of 1.46 μm and 1.15 μm respectively)

Material	Thickness	Depth	Doping	Index (1550 nm)
InGaAs	40 nm	0.04 μm	P 1e19	3.6
InP	1 μm	1.04 μm	P 4e17	3.16
InP	0.15 μm	1.19 μm	undoped	3.17
Q1.46	0.275 μm	1.465 μm	undoped	3.466
InP	0.01 μm	1.475 μm	undoped	3.17
Q1.15	1.2 μm	2.675 μm	N 1e18	3.31
InP	0.5 μm	3.175 μm	N 1e18	3.16
InP	350 μm +/- 25 μm		3~8e18	3.17

To facilitate the optimal coupling to single mode fiber, an experiment was accomplished to test the fiber coupling with different lensed fiber tip spot sizes. It was found that, for

the 2.5 μm mesa width, an optimal coupling was achieved with lensed fiber with a spot size of larger than 4 μm. Thus the optimal coupling can be obtained with the mesa width made closer to the same spot size. This is why the 4 μm wide mesa was chosen, as shown in figure 1, for the Lockheed Martin devices. Because of the frequency requirement, the capacitance of the modulator was limited by the mesa width and length, as the thickness of the Q1.46 is separately determined from desired modulation efficiency. Device lengths of 180 – 200 μm were targeted in the fabrication run. In order to fit the microwave electrodes in a small space, the ground signal electrode configuration was used, as depicted in figure 2. Figure 3 shows a photograph of the wire-bonded EAM.

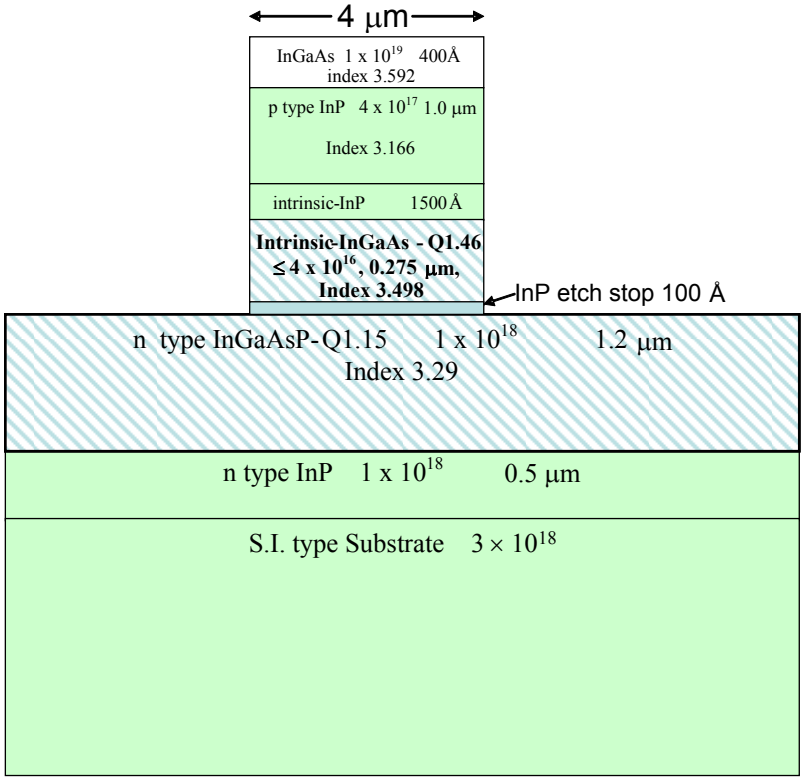

Figure 1 Device cross-section of the diluted waveguide EAM made from materials shown in Table 1

In the course of the project, the thickness of the Q1.46 was modified to 0.375 μm, while the Q1.15 layer was increased to 2 μm, in order to better couple to the lensed fiber. The resulting EAM has a reverse-breakdown voltage in excess of 15 V and a V_π of 3 V for a ~200 mm long waveguide. The device can withstand up to 100 mW of input optical

power with a lowest fiber-to-fiber insertion of 5.5 dB, and a single-octave spurious free dynamic range in excess of 120 dB in a one hertz bandwidth.[2]

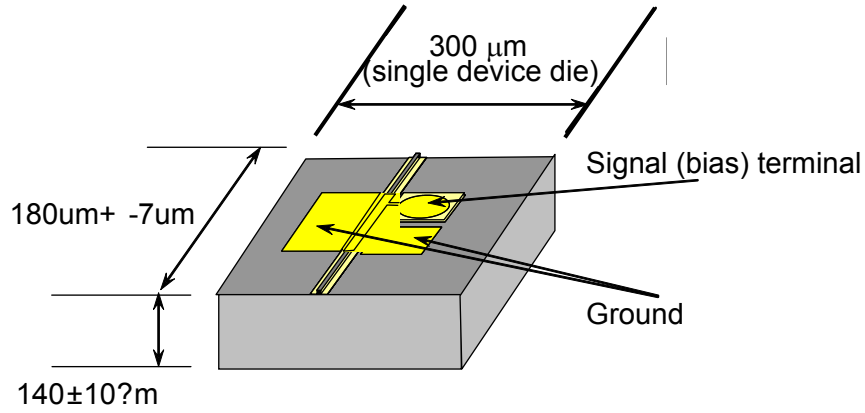

Figure 2 Schematic view of the EAM with the ground-signal electrode configuration.

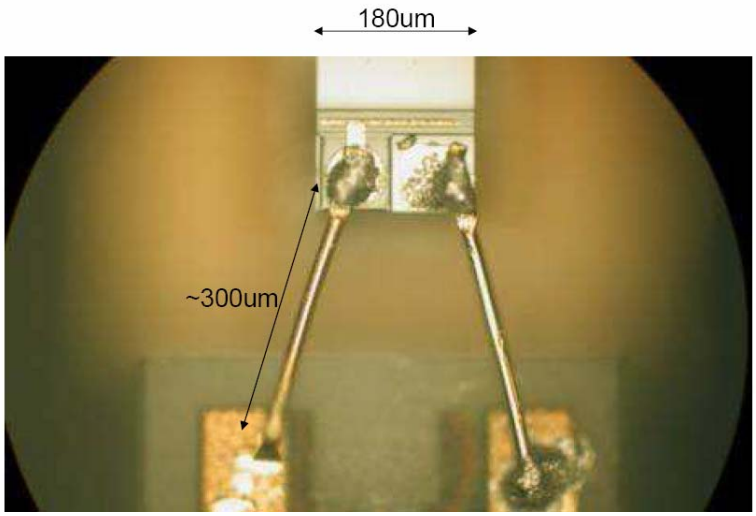

Figure 3 Photograph of the wire-bonded EAM.

Modeling of the microwave electrode – It was determined that the text book type microwave equivalent circuit model of the EAM waveguide does not work well for the current devices due to the ideal circuit elements assumed in the model. Instead, to

[2] EAM results measured at Lockheed Martin.

correlate the experimental measured microwave loss and index with the theory, there is a need to develop an analysis that is based on the physical structure and materials properties of the EAM.

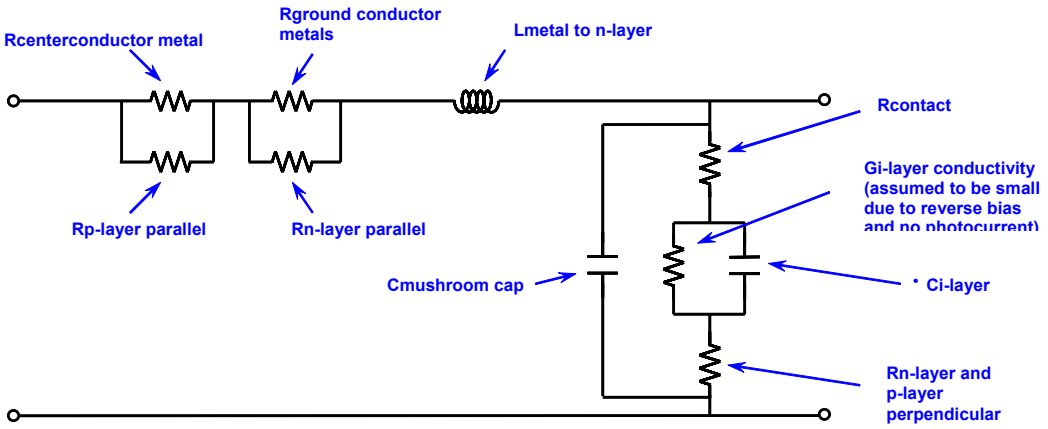

Figure 4 A practical equivalent circuit model of the EAM

This model, as depicted in figure 4, assumes that all of the components are at least, in some capacity, functions of frequency based on the effects of skin effect in each of the conductive materials. The calculated impedances for a 2 μm wide microwave waveguide from the model match very well the measured values (see figures 5a and 5b).

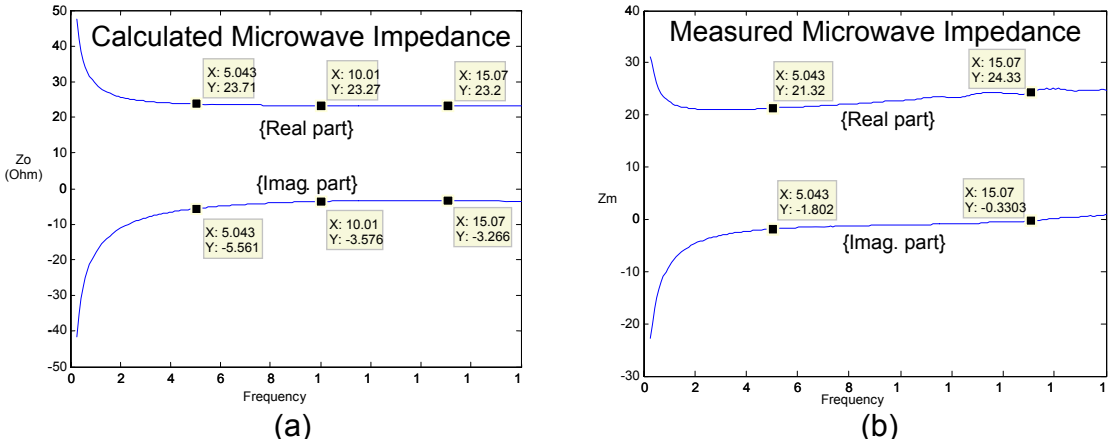

Figure 5 Calculated and measured μ wave impedance for 2μm wide waveguide EAM

It should be noted the measured 2 μm wide microwave waveguide structure yields about 3dB/mm excluding the minor portion due to the probe pad transitions. This results in a small microwave loss for the short EAM waveguide used.

4.2 RF link gain and noise figure limits of electroabsorption modulator

In an external modulation analog link, it is customary to treat the modulator as an ideal three-terminal device where the light is controlled by the voltage applied to the modulator, but there is no effect of the light on the voltage. This assumption is appropriate for modulators where the modulation is based on the linear electro-optic effect. For direct modulation links, the light is produced by the current supplied to the transmitter laser, so there is a direct relation between electrical power supplied to the optical transmitter and the light output. This results in a limitation on the gain of direct modulation links that does not exist for external modulation links [1].

Electroabsorption modulators are intermediate between these two extremes. They are external modulators and they affect the light through voltage-controlled absorption. However, the absorption produces photocurrent, which interacts with the electrical circuit. At low optical power the electroabsorption modulator behaves like an ideal external modulator, but at high optical power it exhibits a gain limit.

This effect of photocurrent on gain was noticed when electroabsorption modulators began to be able to handle optical powers of several mW [2]. This led to the observation that there was a limit on the modulation efficiency of the electroabsorption modulator as the optical power increased [3]. The origin of this limit and how it limits the performance of analog links using electroabsorption modulators was investigated. Experimental data confirming the link gain limit at very high optical power levels was shown.

The basis for this analysis is the equivalent circuit shown in figure 6 where the photocurrent effect is represented by a resistor because it is a voltage-dependent current. The ac voltage on the modulator is v_m. The analysis is simplified by setting $C_M = 0$.

Looking only at the low-frequency effects of the photocurrent the gain limit in its simplest form can be seen. When $C_M \neq 0$, the photocurrent has additional effects such as increasing the 3-dB bandwidth [2], but it does not change the basic effect.

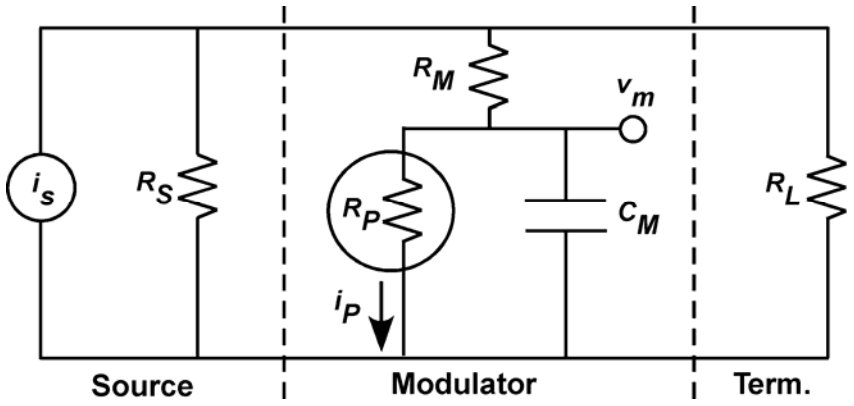

Figure 6 Small-signal ac equivalent circuit of electroabsorption modulator. The resistor R_P represents the voltage-dependent modulator photocurrent source.

This model considers only two sources of loss: voltage-independent coupling losses (t_I and t_O), and voltage-dependent absorption loss. The optical power in the modulator input waveguide is $p_{IN} = p_L t_I$, where p_L is the input laser power. The optical power in the modulator output waveguide is p_{OUT}. This analysis applies to small signals with ac voltage much less than V_π. The equivalent circuit can be solved to give the modulator voltage v_m in terms of the source current i_s as

$$v_m = i_s \frac{R_L R_S}{R_L + R_S} \frac{1}{1 + \frac{p_L t_I \eta_M \pi}{2V_\pi}\left(R_M + \frac{R_L R_S}{R_L + R_S}\right)} \tag{1}$$

where R_L is the modulator termination resistance, R_S is the source impedance, R_M is the resistance in series with the modulator junction, and η_M is the modulator responsivity at the bias point. The link gain is the ratio of the output RF power to the input RF power. The input RF power is defined as the power delivered by the source to a matched load, which is the available power $\langle i_s^2 \rangle R_S/4$. The link output is the power delivered to the detector load resistance R_D.

Under the assumption that there are no losses in the link except the modulator, the link gain is given by eq. 2,:

$$g = \left[\left(\frac{p_L t_I t_O \eta_D \pi}{2V_\pi}\right)^2 R_D R_L\right]\left[\frac{4R_L R_S}{(R_L+R_S)^2}\right]\left[\frac{1}{1+\frac{p_L t_I \eta_M \pi}{2V_\pi}\left(R_M+\frac{R_L R_S}{R_L+R_S}\right)}\right]^2 \quad (2)$$

where η_D is the detector responsivity. The gain is the product of three terms: the link gain for an external modulation link with impedance-matched input, the effect of an impedance mismatch between the source and termination, and a last term with the dependence on the input optical power. In the limit of small p_L, this term approaches unity and the link behaves as expected for an external modulation link.

In the limit of large p_L, the third term becomes inversely proportional to p_L. In this limit the gain becomes independent of either p_L or V_π, and is given by

$$g_{Limit} = \left(\frac{t_O \eta_D}{\eta_M}\right)^2 \frac{4\frac{R_D}{R_S}}{\left(1+\frac{R_M}{R_S}+\frac{R_M}{R_L}\right)^2} \quad (3)$$

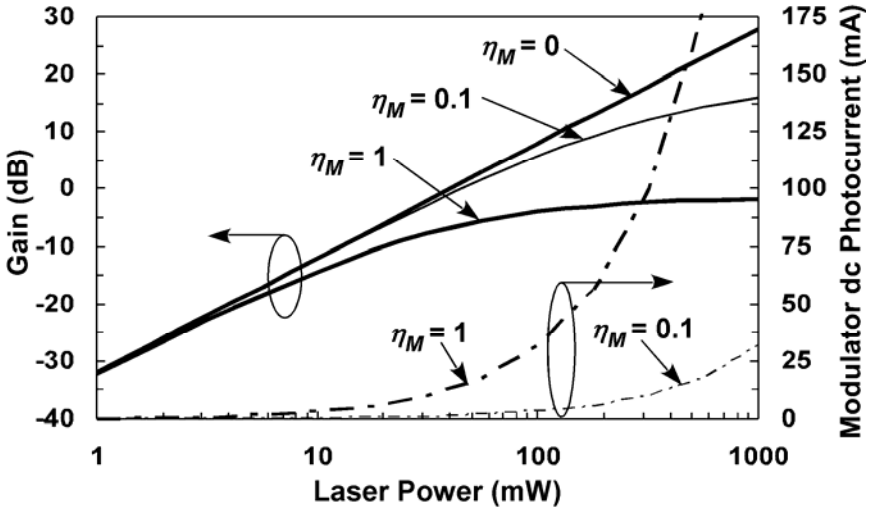

Figure 7 Link electrical gain as a function of laser power, for various values of the modulator responsivity η_M (A/W). The dc component of the modulator photocurrent is also plotted. The parameter values are: V_π = 1 V, $R_S = R_L = R_D$ = 50 Ω, R_M = 5 Ω, η_D = 0.8 A/W, t_I = -2 dB, t_O = -2 dB, and t_B = 0.5. [4]

The effect of this gain limit is shown in figure 7 [4]. The case of $\eta_M = 0$ is the standard external modulation result with no photocurrent effect. The case with $\eta_M = 1$ A/W approximates performance expected from a high-power electroabsorption modulator. For a high-performance modulator the limiting value is near 0 dB. The limit can be increased if the modulator responsivity is reduced.

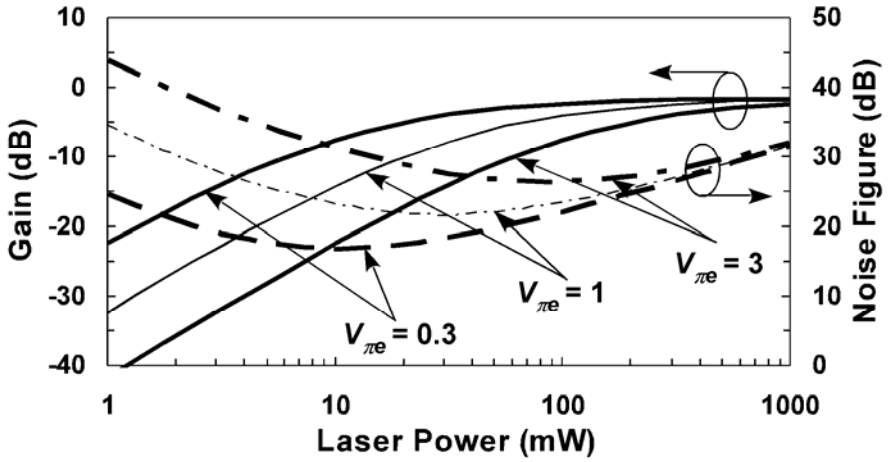

Figure 8 Effect of equivalent V_π on gain and noise figure. The modulator responsivity is 1 A/W. Other parameters are as in Fig. 7.

The gain limit also results in a minimum noise figure. The link electrical noise figure is given by:

$$f = \frac{N_{out}}{gkT_o} = 1 + \frac{f_R}{g} + \frac{2ep_L t_I t_B t_O \eta_D R_D}{gkT_o} + \frac{ep_L t_I \eta_M (1 - t_B) R_S \left[1 + \frac{R_M (R_L + R_S)}{R_S R_L}\right]^2}{2kT_o} \quad (4)$$

where N_{out} is the total output noise, f_R is the receiver noise figure ($f_R = 1$ in this case), k is Boltzmann's constant, T_o is 290K, and e is the elementary charge. The first three terms are the familiar input, receiver, and detector shot noise terms. The fourth term is due to shot noise from the dc component of the modulator photocurrent. For small η_M or for low bias (small t_B) the modulator shot noise term becomes the dominant term at high optical power. The noise figure is plotted in figure. 8.

The gain limit has been verified by measuring the gain of a link using an electroabsorption modulator at high optical power levels. The modulator equivalent V_π was 0.85 V and the input and output losses were approximately $t_I = t_O = 0.5$. The bias point was $t_B = 0.5$, which occurred at 1.5 V reverse bias. The ac input voltage was 0.063 V peak-to-peak. The modulator's apparent dc responsivity varied from 0.7 to 1.5 A/W, indicating some mechanism creating additional photocurrent beyond simple absorption. An RF responsivity, $\eta_M = 0.8$ A/W, was used to fit the calculation to the measured data. The measurement frequency was 50 MHz, well below the RC bandwidth.

The results are shown in figure 9. The gain follows the theoretical prediction very closely. The gain deviates from the prediction of this model only at the highest powers used (>250 mW) due to heating.

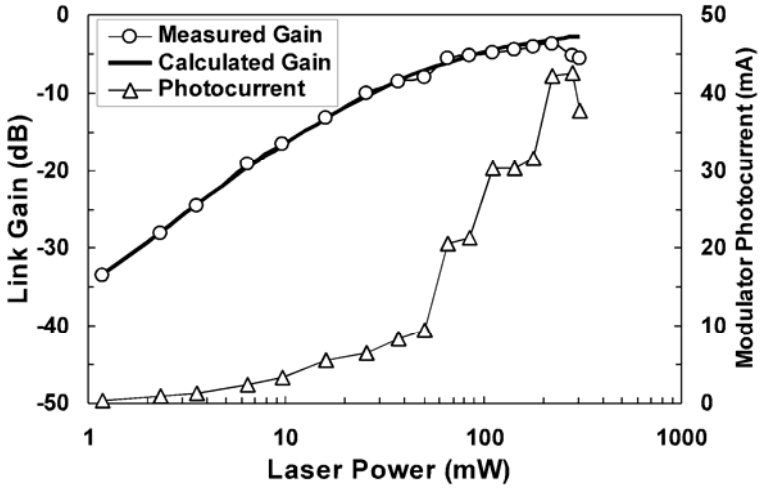

Figure 9 Experimental measurement of a link using an EAM modulator at 1550 nm, compared with the theoretical gain calculation.

4.3 Limit of Spurious free dynamic range of electroabsorption modulator

The main conclusion from Section B.2 was that the voltage reduction across the p-i-n junction, due to the negative feedback effect generated by the photocurrent, causes link gain to deviate from the quadratic dependence on input optical power and finally

approach a gain limit. Here it is shown that the same mechanism affects EAM linearity as well. The linearity performance solely due to the photocurrent feedback effect was analyzed. The results show an input third-order intercept point (IIP3) dependence on fourth-order power of optical power at substantially high power, which surpasses the increase in noise which is linearly dependent on optical power. The SFDR of the link is thus anticipated to improve with increased optical power.

While the input optical power is increased, both dc and ac photocurrent generation increases as well. As a result, voltage drop on the source resistance R_S and serial resistance R_M takes more portion of the total source voltage, leaving less modulation voltage on the p-i-n junction. From a feedback point of view, what happens in the EAM resembles a negative feedback system. The incoming voltage v_S modulates the junction and produces intensity modulation of optical carrier $P_L t_I t_P t_O[T(V_B)\text{-}T(V_B+v_M)]$, where $T(V)$ is the optical transfer function of the EAM. At the same time, the modulated light generates an ac photocurrent. The ac photocurrent effectively reduces the voltage across the junction. This is effectively a negative feedback system with the output coupled into the photodetector and generates an output voltage v_L across load resistance R_D. When the input optical power is low, the photocurrent feedback can be ignored and the linearity of electro-to-optical conversion is determined by the optical transfer function $T(V)$. When the optical power increases, the effective voltage across EAM junction is no longer v_S, but v_M which is modified by photocurrent feedback.

By using a voltage gain function $v_{OUT} = g(v_{IN})$ without feedback, v_{IN} and v_{OUT} under feedback can related as follows.

$$g\left(v_{IN} - f v_{OUT}\right) = v_{OUT} \tag{5}$$

where g is a function including nonlinear harmonics caused by optical transfer curve $T(V)$, and f is the negative feedback coefficient related to the modulator parameter and the remote resistor. It should be noted that $v_{IN} = v_S/2$ so as to conform with the conventional definition of fiber-optic link gain, where the input RF power is taken with a modulator

load matched to the source [5].

The output voltage v_{OUT} is equivalent to v_L, the ac voltage across the load resistance of the photodetector. It is well known in electronic amplifier design that negative feedback can improve the linearity of the whole system if the feedback coefficient is more linear than the transfer function of the system without feedback [6]. When the loop voltage gain is large, the overall feedback system response is close to an inverted feedback network response. In this case, function *g* includes optical transfer curve nonlinearities. However, feedback coefficient *f* has nothing to do with the nonlinear transfer curve. When the voltage gain without feedback is high enough, the voltage gain can be approximated as 1/*f*. The system linearity is therefore determined mainly by *f*, not the EAM transfer function. The EAM and photodetector responsivities η_M and η_D involved in *f* can still affect the system linearity.

The impact of this fiber-optic link linearity by photocurrent feedback can also be analyzed by separating intrinsic and extrinsic optical transfer curves. The intrinsic optical transfer curve is defined as a function of junction voltage $T(V_M)$. It is clear that the aforementioned optical transfer curve is equivalent to the intrinsic optical transfer curve definition. Also the extrinsic optical transfer curve is then defined dependent on $v_{IN} = v_S/2$, $Te(V_{IN})$. The extrinsic optical transfer curve includes negative photocurrent feedback effect and governs the linearity when the EAM gain is saturated. Different orders of derivatives of both intrinsic and extrinsic optical transfer curves with respect to their arguments can be evaluated and related based on the EAM equivalent circuit model; for instance:

$$\frac{dT_e}{dV_{IN}} = \frac{2\dfrac{dT}{dV_M}}{1 - P_L t_I t_P \eta_M \left(R_S + R_M\right)\dfrac{dT}{dV_M}} \tag{6}$$

Equation (6) is the relationship between first order derivatives of the transfer curves. It accounts for the link gain saturation. The term dT/dV_M is considered negative due to the fact that larger voltage causes less optical transmission. The denominator on the right hand of (6) becomes much larger than unit when the input optical power is high enough, which reduces the link gain. It can be lump as an EAM saturation factor *k*.

$$k = 1 - P_L t_I \eta_M (R_S + R_M) \frac{dT}{dV_M} = 1 + \frac{P_L t_I \eta_M (R_S + R_M)\pi}{2V_\pi} \quad (7)$$

The derivatives of extrinsic and intrinsic optical transfer curves are related by a factor of k^3 for the second order, and k^4 for the third order when the EAM is biased at its largest slope efficiency voltage point where second order derivative nulls out. The second order null point is also the bias point for multi-octave operation. It is clear that the derivatives of extrinsic optical transfer curves become much smaller than that of intrinsic optical transfer curves when saturation factor k>>1.

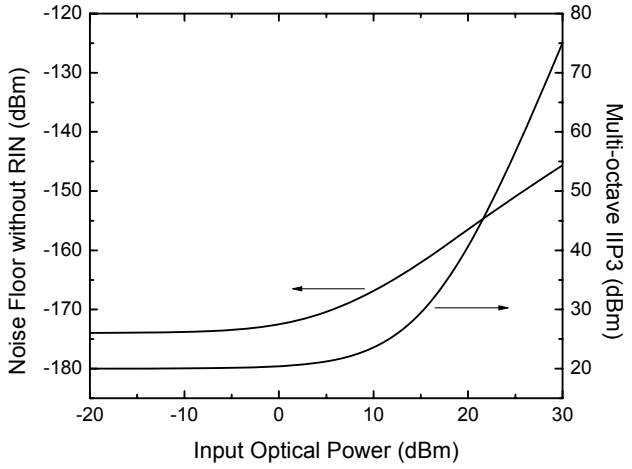

Figure 10 Calculated link output noise floor and multi-octave IIP3 of EAM as a function of input optical power. Laser RIN noise is not included. Low power EAM IIP3 of 20 dBm is assumed. Extra optical loss caused by dc bias of EAM is 3 dB. Other parameters used in the calculation are: $t_I = t_O$ = 0.5, t_P = -1 dB, $R_S = R_D$ = 50 Ω, R_M = 5 Ω, $\eta_M = \eta_D$ = 1 A/W, V_π= 1.5 V.

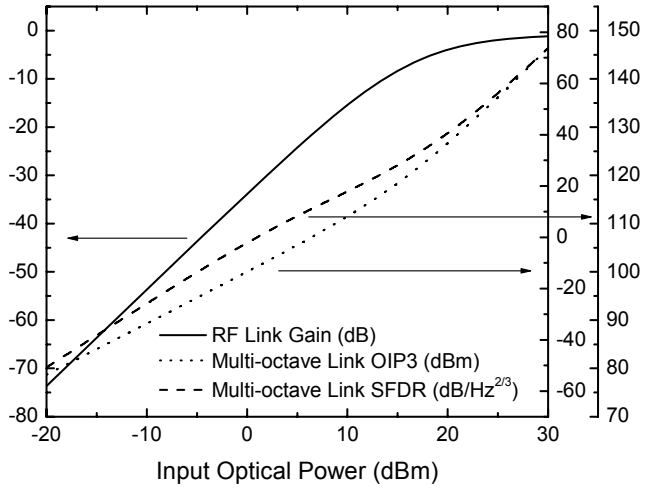

Figure 11 Calculated RF link gain, multi-octave link OIP3 and SFDR dependence of EAM on input optical power.

Thus it can be see that the IIP2 and IIP3 of a highly saturated EAM link can be improved by a factor of k^4 compared with non-feedback system, as illustrated in figures 10 and 11. The output second and third-order intercept points (OIP2 and OIP3) increase by the same factor as the gain saturates. On the other hand, the link output noise only increases linearly with optical power, even when EAM shot noise dominates in the saturation case, which is approximately proportional to k. Here laser relative intensity noise (RIN) is excluded. Therefore link SFDR also improves by k^2 under this situation.

5. Conclusion and future plan

Under the support of the Air Force Research Laboratory, much progress has been made in this effort in the fabrication of the diluted core waveguide electroabsorption modulator for analog fiber links. Notable progress has been made in the understanding of the performance of electroabsorption modulator for analog applications. Further effort is planned to show that RF fiber optic links using an EAM in the transmitter can achieve large SFDR operation in a demonstration set-up.

6. References.

1. C.H. Cox III, *Analog Optical Links: Theory and Practice*, Cambridge University Press, 2004, Ch. 3.
2. G.L. Li, C.K. Sun, S.A. Pappert, W.X. Chen, and P.K.L. Yu, "Ultrahigh-speed traveling-wave electroabsorption modulator—design and analysis," *IEEE Trans. Microwave Theory Tech.*, vol. 47, pp. 1177-1183, July 1999.
3. L.A. Johansson, Y.A. Akulova, G.A. Fish, and L.A. Coldren, "High optical power electroabsorption waveguide modulator," *Electron. Lett.*, vol. 39, pp. 364-365, 20 Feb. 2003.
4. G. E. Betts, X. Xie, I. Shubin, W. S. C. Chang, and P. K. L. Yu, "Gain Limit in Analog Links using Electroabsorption modulator," *IEEE Photonics Technology Letters,* Vol. 18, No. 19, pp. 2065-2067-1542, 2006.
5. C. H. Cox III, E. I. Ackerman, G. E. Betts, and J. L. Prince, "Limits on the performance of RF-over-fiber links and their impact on device design," *IEEE Trans. Microwave Theory and Tech*., vol. 52, no. 4, pp. 906–920, Feb. 2006.
6. T. H. Lee, *The Design of CMOS Radio-Frequency Integrated Circuits*. Cambridge, U.K.: Cambridge Univ. Press, 1998, ch. 14.

7. Glossary for Acronym

EAM = Electroabsorption modulator

IIP3 = input third-order intercept point

OIP3 = output third-order intercept point

RF = Radio Frequency

SFDR = Spurious Free Dynamic Range

UCSD = University of California, San Diego

V_π = half wave voltage; voltage to generate a π phase shift

Appendix: Publications

1. G. E. Betts, X. Xie, I. Shubin, W. S. C. Chang, and P. K. L. Yu, "Gain Limit in Analog Links using Electroabsorption modulator," *IEEE Photonics Technology Letters,* Vol. 18, No. 19, pp. 2065-2067-1542, 2006.
2. P. K. L. Yu, I. Shubin, X.B. Xie, W. S. C. Chang, "Recent Advances in Photonic Devices for RF/Wireless Communication Applications" invited presentation, to be presented at the 12th Microcoll Conference at Budapest, Hungary, May 2007.
3. X. B. Xie, I. Shubin, W. S. C. Chang, and P. K. L. Yu, "Analysis of Linearity of Highly Saturated Electroabsorption Modulator Link due to Photocurrent Feedback Effect", to be submitted to Optics Express.